RET overactivation leads to concurrent Hirschsprung disease and intestinal ganglioneuromas

Nandor Nagy[1], Richard A. Guyer[2], Ryo Hotta[2], Dongcheng Zhang[3], Donald F. Newgreen[3], Viktoria Halasy[1], Tamas Kovacs[1], Allan M. Goldstein[2,*]

[1] Department of Anatomy, Histology and Embryology, Faculty of Medicine, Semmelweis University, Budapest, Hungary

[2] Department of Pediatric Surgery, Massachusetts General Hospital, Harvard Medical School, Boston, MA, USA

[3] Neural Crest Group, Murdoch Children's Research Institute, Parkville, Australia

Keywords: enteric nervous system, aganglionosis, ganglioneuroma, multiple endocrine neoplasia, GDNF, Hirschsprung disease

*Corresponding author:

Allan M. Goldstein

Massachusetts General Hospital

55 Fruit St., WRN 1151, Boston, MA 02114

E-mail address: agoldstein@partners.org

Phone: 617-726-0270

Summary statement

This study reveals novel evidence that excess GDNF-RET signaling can lead to phenotypic diversity in the enteric nervous system, including both aganglionosis and intestinal ganglioneuromas.

Abstract

Appropriately balanced RET signaling is of critical importance during embryonic neural crest cell migration, proliferation, and differentiation. RET deficiency, for example, leads to intestinal aganglionosis (Hirschsprung disease), while overactive RET can lead to multiple endocrine neoplasia (MEN) syndromes. Some RET mutations are associated with both intestinal aganglionosis and MEN-associated tumors. This seemingly paradoxical occurrence has led to speculation of a "Janus mutation" in RET that causes overactivation or impairment of RET activity depending on the cellular context. Using an intestinal catenary culture system to test the effects of GDNF-mediated RET activation, we demonstrate the concurrent development of distal colonic aganglionosis and intestinal ganglioneuromas. Interestingly, the tumors induced by GDNF stimulation contain enteric neuronal progenitors capable of reconstituting an enteric nervous system when transplanted into a normal developmental environment. These results suggest that a Janus mutation may not be required to explain co-existing Hirschsprung disease and MEN-associated tumors, but rather that RET overstimulation alone is enough to cause both phenotypes. The results also suggest that reprogramming tumor cells toward nonpathological fates may represent a possible therapeutic avenue for MEN-associated neoplasms.

Introduction

GDNF and its tyrosine kinase receptor, RET, are among the most important signaling pathways during enteric nervous system (ENS) development. During ENS formation, GDNF in the gut mesenchyme binds to a receptor complex formed by Ret and its co-receptor, GDNF family receptor α1 (GFRα1), both present on enteric neural crest-derived cells (ENCCs), to promote their survival, proliferation, migration, and differentiation (Heuckeroth et al., 1998; Taraviras et al., 1999; Young et al., 2001). Loss-of-function mutations in GDNF, GFRα1, or RET lead to intestinal aganglionosis in mice (Goldstein et al., 2013) and humans (Amiel et al., 2008). Mutations which impair RET signaling cause Hirschsprung disease (HSCR) due to failure of ENCCs to migrate, proliferate, and/or differentiate properly within the intestine (Brooks et al., 2005). In contrast, mutations leading to constitutively active RET are implicated in two distinct multiple endocrine neoplasia (MEN) syndromes, which are associated with the development of tumors: MEN2A is characterized by medullary thyroid cancer, pheochromocytomas, and hyperparathyroidism, and MEN2B consists of medullary thyroid cancer, pheochromocytomas, and ganglioneuromas of the gastrointestinal tract (Hansford and Mulligan, 2000). Ganglioneuromas are benign tumors that occur primarily in the submucosa and lamina propria of the intestine and represent hamartomas containing neuronal and glial elements (Hechtman and Harpaz, 2015). Understanding biologic processes mediated through RET is thus relevant both for understanding normal and abnormal development and for developing novel therapies for these conditions.

MEN2A and MEN2B are caused by distinct types of RET mutations (Arighi et al., 2005; Plaza-Menacho et al., 2007). MEN2A is associated with extracellular domain mutations in conserved cysteine residues that cause dimerization and internalization of constitutively active RET (Eng et al., 1996; Mulligan et al., 1993). In contrast, intracellular mutations within the tyrosine kinase domain that cause constitutive signaling from RET monomers are found in MEN2B (Menko et al., 2002). While both diseases are associated with exuberant RET activity, MEN2A is known to be associated with HSCR (Cohen et al., 2002; Takahashi et al., 1999). Gastrointestinal symptoms are common in patients with MEN2B, including constipation, pseudo-obstruction, and megacolon, and are likely due to the development of intestinal ganglioneuromas (Cohen et al., 2002), with only one reported case of HSCR in a patient with MEN2B (Romeo et al., 1998). Because the disease phenotypes of the two MEN syndromes differ, the associated RET mutations must impact cells in disparate ways.

Understanding this biology and developing new therapies requires accessible and reproducible mammalian model systems for modulating RET signals in biologically meaningful contexts that reproduce the phenotypes observed in humans.

A major challenge in understanding the occasional coexistence of HSCR and MEN is that the former is due to loss of RET activity whereas the latter is caused by its overactivation. This paradox has led to the concept of "Janus mutations," single mutations in RET capable of causing both increased and decreased signaling depending on its cellular context (Arighi et al., 2004; Moore and Zaahl, 2010). However, evidence for the existence of such mutations is limited to *in vitro* signaling studies (Arighi et al., 2004). Models that recapitulate clinical phenotypes are challenging to develop. Cell culture systems lack the cellular diversity and complex spatial relationships found in multicellular organisms. Animal models, such as targeted- and conditional-knockout mice, can faithfully recapitulate disease, but are costly and time consuming to create. Drosophila models harboring MEN2-associated RET mutations have been used to identify signaling pathways involved in MEN2 pathogenesis, such as the Ras-ERK and Src pathway, but differences between mammalian and insect physiology call into question the relevance of these systems to the human disease (Read et al., 2005; Vidal et al., 2005). We report here a catenary culture model of RET overactivation in both chick and mouse embryonic gut. This model recapitulates aspects of both MEN syndromes and HSCR, with development of intestinal ganglioneuromas and failed migration of ENCCs to the distal hindgut. The results allow us to generate hypotheses on how RET overactivation can lead to this phenotypic diversity.

Results

Intestine, including midgut and hindgut, was explanted from E7 chick, a stage at which rostrocaudal ENCC migration has reached the mid-hindgut. Under control conditions, over the ensuing 48 hours, ENCCs will complete migration to the terminal end of the hindgut and pattern a normal ENS in the submucosal and myenteric plexuses (Nagy et al., 2016). After removal of the nerve of Remak and cloaca, explants were placed in catenary cultures for 48 hours in media containing 40 ng/ml GDNF (Fig. 1A). The catenary culture is an *ex vivo* organotypic culture in which the gut is pinned at its ends and floating along its length without attachment of the gut to the culture surface. This is useful in studying ENS migration as it

minimizes outward migration of ENCCs from the gut and onto the surrounding matrix environment. After 48 hours in culture, large cellular aggregates formed on the surface of the gut (Fig. 1B, arrows). These aggregates occurred mostly in the ceca and post-umbilical midgut. The aggregates were comprised of enteric neurons that stain for Tuj1 (Fig. 1C-E), Hu (Fig. 1G,H), and neurofilament (Fig. I), and contained actively proliferating cells, as shown by EdU incorporation (Fig. 1E). The aggregates also contained Sox10+ (Fig. 1F,G) and BFABP+ (Fig. 1H) enteric glia, but no SMA+ smooth muscle cells (Fig. 1J). Fibronectin expression was absent (Fig. 1K), while Tenascin-C, which is produced by ENCCs (Akbareian et al., 2013), was strongly expressed (Fig. 1L). To determine what happens to these large ENCC aggregates over time, E6 midgut was cultured in the presence of GDNF for 48 hours and then transplanted onto the CAM of a normal host chick embryo for 7 days. This method allows a longer culture period so that we can assess the long-term effect of that 48-hour GDNF treatment on the ENS. Guts treated with GDNF have hyperplastic enteric ganglia in both the submucosal and myenteric plexuses with significantly increased interganglionic fibers (Fig. 2A,A') as compared to a CAM-grafted intestine that was not treated with GDNF (Fig. 2B,B').

The catenary culture experiments were repeated using E11.5 mouse gut and, as with the chick intestine, GDNF similarly induced the formation of numerous, large cellular aggregates on the gut surface (Fig. 3A, arrows). Aggregates were again located primarily in the midgut and cecum. These were highly enriched for RET+/p75+ neural crest-derived cells (Fig. 3B-D), with active cell proliferation (Fig. 3D). They also contained a high density of enteric neurons, expressing Hu (Fig. 3E), neurofilament (Fig. 3F), PGP9.5 (Fig. 3G), and synaptophysin (Fig. 3H,H'). The aggregates expressed BFABP (Fig. 3I) and S100 (Fig. 3J), indicating the presence of glial precursors. GFAP, a marker of mature enteric glia, was absent (Fig. 3K), consistent with the fact that GFAP is normally not expressed until E16.5 in the mouse ENS (Young et al., 2003). SMA was not expressed in the aggregates (Fig. 3L). Aggregates were then dissociated and the ENCCs plated onto a fibronectin-coated surface in media containing GDNF, where they undergo extensive cellular proliferation (Fig. 3M).

As with E7 chick gut above, culturing E6 gut for 2 days in the presence of GDNF resulted in similar ENCC aggregates in the midgut (Fig. 4A, black arrows). These aggregates form both on the gut surface (Fig. 4A) and within the mesenchyme (Fig. 4B), with the majority of cells expressing N-cadherin (Fig. 4C), a marker of undifferentiated and differentiated ENCCs

(Nagy et al., 2012). These aggregates contain highly proliferative cells that incorporate EdU (Fig. 4C), and many of these EdU+ cells Sox10+ and BFABP-negative (Fig. 4F-I"), consistent with an ENCC progenitor population. Given the location and immunophenotype of the cell clusters, we refer to them as "ganglioneuromas." Of note, ENCC migration, which is normally at the level of the cecal-midgut junction at E6 and migrates well into the distal hindgut after 48 hours in control conditions (Fig. 4D, arrowheads), is arrested in the presence of added exogenous GDNF, with no cell migration beyond the most proximal hindgut (Fig. 4B, arrowheads). Interestingly, addition of GDNF to E9 intestine did not result in ganglioneuroma formation (Supplemental Fig. 1), suggesting a stage-specific effect of Ret overactivation. Furthermore, ENS migration was normal in these E9 guts, as would be expected given that ENCC migration is completed by E8 in the chick intestine.

We next performed a series of experiments to explore the concentration-dependent and time-dependent relationship between GDNF concentration and ganglioneuroma number and size. We also examined whether the concentration of GDNF impacted ENS colonization of the hindgut. E7 chick intestine was cultured in catenary conditions for 72 hours with GDNF concentration ranging from 0 to 500 ng/ml. GDNF-induced ganglioneuromas are clearly visible on the surface of the gut (Fig. 5C,E,G,I). Longitudinal sections stained with N-cadherin show a normal ENS in the control gut (Fig. 5B), with numerous and large ganglioneuromas following GDNF treatment (Fig. 5D,F,H,J). Of note, ganglioneuromas are visible on the surface of the midgut but not the hindgut. In contrast, intramural ganglioneuromas are present throughout.

The effect of GDNF concentration on extent of hindgut aganglionosis was examined in E7 intestine cultured in catenary conditions in the presence of varying concentrations of GDNF for 72 hours. Longitudinal sections were stained with N-cadherin and the length of distal hindgut lacking ENS was measured from the position of the distalmost ENCC or ganglioneuroma to the end of the cloaca. As shown in Fig. 5K, the addition of exogenous GDNF inhibits ENCC migration, with the control group exhibiting significantly less aganglionosis than each of the four treatment groups ($p<0.05$). This difference was concentration dependent, with the 10 ng/ml treatment group having less aganglionosis than both the 100 ng/ml and 500 ng/ml treatment groups ($p<0.05$).

Since a known cause for distal intestinal aganglionosis in HSCR is the premature differentiation of ENCCs, we quantified the proportion of neurons in the hindgut of control versus GDNF-treated guts. As shown in Fig. 5L, GDNF treatment resulted in a 24% increase in total ENCC number as compared to control (21.6±1.5 v. 17.4±5.0 cells per 40^{o} arc of cross-section, $p<0.05$). In addition, the number of Hu-expressing enteric neurons also increased significantly (11.0±0.9 v. 7.1±0.5, $p<0.001$). This represents a 25% increase in the proportion of ENCCs that were differentiated enteric neurons (51.0% v. 41.0%). In contrast, the number of SoxE+ cells, which represent ENCC progenitors and enteric glia, but not differentiated neurons, was unchanged (10.6±0.8 v. 10.3±0.5).

The number of ganglioneuromas was counted per gut and normalized to the length of the intestine. As shown in Fig. 5M, ganglioneuroma number was related to GDNF concentration, with the fewest number seen at 10 ng/ml GDNF and the greatest number occurring at 500 ng/ml (Fig. 5M). The difference between 500 ng/ml and each of the three other treatment groups was statistically significant ($p<0.05$). Ganglioneuroma number, however, did not increase significantly over time. Ganglioneuroma size was also dependent on GDNF concentration, with the smallest ganglioneuromas occurring at 10 ng/ml GDNF and larger ganglioneuromas seen at 40-500 ng/ml (Fig. 5N). The differences between 10 ng/ml and the other three treatment groups were all statistically significant ($p<0.05$). Notably, ganglioneuroma size increased over time, with statistically significant differences seen between 24 and 48 hours ($p<0.05$) and between 24 and 72 hours ($p<0.05$). The lack of substantial increase in ganglioneuroma number over time and the fact that their size does not increase substantially after 48 hours may be explained by the fact that ganglioneuromas were counted and measured on the gut surface. By around the second day of culture, however, large ganglioneuromas often spontaneously detach from the surface while smaller ones appear.

To identify the cell of origin for the ganglioneuromas and exclude the possibility that they arise from remnants of the nerve of Remak (an avian-specific structure arising from sacral neural crest and consisting of a chain of ganglia adjacent to the gut from the midgut to the cloaca) due to its incomplete removal from the chick intestine, GFP-expressing plasmid was electroporated into either the vagal or sacral level of the neural tube at E1.5 or E2.25, respectively. The intestines were explanted at E6.5-E7 with the nerve of Remak intact and the cloaca removed. Note that at this stage sacral ENCCs are not present in the gut because they have not yet entered the hindgut from the peri-cloacal pelvic plexus (Nagy et al., 2007). Guts

were maintained in organotypic culture for an additional 48 hours with or without added GDNF. Control guts, in which the vagal neural tube was electroporated with GFP plasmid and to which GDNF protein was not added, show GFP-expressing ENCCs throughout the ENS and no abnormal aggregate formation (Fig. 6, left column). Treatment with GDNF results in large ganglioneuromas containing double-expressing GFP+ vagal crest-derived cells and Hu+ enteric neurons in the midgut and ceca (Fig. 6, middle column). In contrast, electroporation of the sacral level neural tube results in GFP+ ENCCs only in the nerve of Remak, confirming successful labeling of sacral neural crest-derived ENCCs (Fig. 6, right column), and not in the gut. While ganglioneuromas form following GDNF treatment of these guts, they do not contain GFP+ cells, suggesting that GDNF-induced ganglioneuromas arise only from vagal ENCCs and not from sacral crest-derived cells. Importantly, addition of GDNF caused significant disruption of ENS structure, with loss of the normal submucosal and myenteric plexuses, especially in the midgut, as shown in Fig. 6, middle row. This finding is consistent with exogenous GDNF disrupting migration and patterning of ENCCs.

To characterize the cell composition of GDNF-induced ganglioneuromas and their developmental potential, E6 gut was harvested from transgenic GFP-expressing chick embryos and cultured with GDNF for 48 hours to form ganglioneuromas. Two ganglioneuromas were removed from these guts and one was implanted into each of the two ceca of an E5 chick gut (Fig. 7A, arrowheads), a stage at which the ENCC wavefront has only reached the distal midgut and the hindgut remains preganglionic. This gut was then cultured on the CAM of an E9 host embryo for 9 days to allow migration of ENCCs out of the ganglioneuromas. As shown in Fig. 7B,C, the ganglioneuromas give rise to a fully colonized ENS in the hindgut, with GFP+ enteric neurons patterning in submucosal and myenteric plexuses (Fig. 7D). The same experiment was repeated with ganglioneuromas derived from E11.5 Wnt1;tdT mouse embryos (Fig. 7E,F), again implanting one mouse-derived ganglioneuroma into each of the two ceca of an E5 chick gut. After 9 days on the CAM, tdT-expressing cells have migrated throughout the hindgut and formed a well-developed ENS (Fig. 7G,H). Wnt1-derived cells express the neuronal markers Hu (Fig. 7H, inset), PGP9.5 (Fig. 7I), and nNOS (Fig. 7J) as well as the glial markers GFAP (Fig. 7K) and S100 (Fig. 7L). The lack of immunostaining for CN (Fig. 7M), a chick-specific neuronal antibody, confirms the mouse origin of the entire ENS. These results show that GDNF-derived ganglioneuromas contain ENCC progenitors capable of giving rise to a normally patterned ENS comprising both neurons and glia.

Discussion

Using organotypic cultures, we show that excess GDNF leads to tumors of the ENS resembling intestinal ganglioneuromas (Hechtman and Harpaz, 2015) and distal intestinal aganglionosis. The occurrence of these two phenotypes seems paradoxical, as the former is generally believed to be due to excess RET signaling while the latter is felt to be caused by RET deficiency. However, our data suggest that the degree of RET stimulation is of fundamental importance to both. Abnormally low RET signaling hinders colonization of the hindgut, as seen in classic HSCR-causing mutations (Brooks et al., 2005). At appropriate levels of RET activity, differentiation and proliferation of ENCCs are balanced properly to support development of a normal and fully colonized ENS. In contrast, exuberant RET activity, such as from MEN-associated RET-activating mutations or excess GDNF as in this study, alters the critical balance of proliferation and differentiation, leading to arrested migration of ENS precursors due to their premature neuronal differentiation, while simultaneously inducing excessive proliferation of RET-responsive cells (Plaza-Menacho et al., 2007). This is consistent with studies conducted using canine kidney cells, which found that the RET-activating, MEN2A-associated C620 mutation causes both increased proliferation and decreased migration of cultured cells (Arighi et al., 2004). In our model, excess GDNF causes premature differentiation and migratory arrest of ENS precursors as well as excessive proliferation of ENCCs that give rise to ganglioneuromas. Hence, the occurrence of this phenotypic diversity in our experimental system suggests that Janus mutations do not necessarily need to be invoked to explain the clinically observed coexistence of HSCR and MEN-associated tumors. However, we acknowledge that our model may not fully recapitulate all aspects of the human disease. First, MEN syndromes are normally associated with RET-activating mutations rather than excess GDNF. Second, interspecies differences in the cellular response to RET activation may be important. Other factors may also influence our results, including the tissue-specificity of RET activation in our culture system and its timing relative to specific developmental events.

Interestingly, the excessive ENCC proliferation we observe leads to large ectopic clusters of cells rather than simply a hyperplastic ENS. As GDNF is an ENCC chemoattractant (Young et al., 2001), we hypothesize that the presence of exogenous GDNF in the culture media may

attract some ENCCs to migrate outward toward the gut surface, leading to ectopic ENCC tumors throughout the mesenchyme, and these grow larger in response to the mitogenic effect of GDNF. Overactivation of RET signaling induces the proliferation of ENCC progenitors, as confirmed by their expression of N-Cadherin, Ret, SOX10, and P75. The GDNF-induced ENS tumors that occur in the developing mouse and chick gut are thus highly enriched for these ENCC progenitors and may serve as a good source of these cells for future studies.

MEN2A, which classically includes medullary thyroid cancer, pheochromocytomas, and hyperparathyroidism, is known to be associated with HSCR (Plaza-Menacho et al., 2007; Takahashi et al., 1999), but not with intestinal ganglioneuromas. MEN2B, on the other hand, has only rarely been reported in a patient with HSCR (Romeo et al., 1998). However, MEN2B is associated with ganglioneuromas and also with a high prevalence of gastrointestinal symptoms, including constipation, dysmotility, and megacolon (Cohen et al., 2002; Romeo et al., 1998). Careful phenotypic analysis of the ENS in MEN2B patients, however, has not been performed and, based on our results, we hypothesize that some of these individuals may have either a short segment of aganglionosis, hypoganglionosis, or other ENS abnormalities in addition to the ganglioneuromas. Intestinal biopsies and histochemical evaluation of the ENS may be warranted to more fully characterize the ENS in these patients.

In our model system, ganglioneuromas only arise if GDNF treatment is applied during colonization of the gut, as evidenced by the lack of tumors seen when E9 tissue is treated. This suggests that the response of ENCCs to GDNF signaling changes after gut colonization is completed, either due to downregulation of its receptor or an intracellular milieu that responds differently to RET activation. In humans, gastrointestinal tract ganglioneuromas associated with MEN have beeen identified from infancy to early adulthood (Erdogan et al., 2006; Smith et al., 1999), but many are asymptomatic and therefore when they first began to develop is unknown. Our embryonic model of ganglioneuroma development may recapitulate what occurs in the human disease, but little is known about the development of these MEN-associated tumors. This model system therefore provides an opportunity to study the origin of intestinal ganglioneuromas in more detail.

Intriguingly, cells isolated from the ganglioneuroma-like structures stimulated by GDNF were able to reconstitute a normal-appearing ENS when transplanted into a normal developmental environment. This suggests that at least some cells contained within the intestinal ganglioneuromas retain a progenitor-like state that can be activated upon introducing them into a normal embryonic milieu. This finding has important implications. First, it suggests that the organotypic culture conditions we used can be leveraged for generating large numbers of progenitor ENCCs for further studies, as mentioned above. Second, other neural-crest derived tumors may also have similar potential for redirection toward non-pathologic fates when placed in the proper conditions. This phenomenon is well described in neuroblastomas, for example, which have a propensity for spontaneous regression (Brodeur, 2018; Matthay et al., 2016). Understanding how tumors can be redirected to nonpathological fates may be useful for developing novel pharmacotherapies.

In conclusion, we demonstrate here the ability of RET overactivation to cause both HSCR and intestinal ganglioneuromas, offering a new model system for studying both conditions. Our results suggest that the coexistence of these two seemingly opposite phenotypes can be explained by excessive RET signaling alone and without invoking a Janus mutation. We have also demonstrated that the cells comprising the ganglioneuroma-like masses induced by RET activation maintain their embryonic potential to generate an ENS, suggesting that these ganglioneuromas, and possibly other MEN-associated neoplasms, may be amenable to reprogramming along normal developmental trajectories.

Materials and Methods

Animals

Fertilized White Leghorn chicken (*Gallus gallus domesticus*) eggs were obtained from commercial breeders and maintained at 37.5 °C in a humidified incubator. Transgenic green fluorescent protein (GFP)-expressing chicken eggs were obtained from Prof. Helen Sang, The Roslin Institute, University of Edinburgh (McGrew et al., 2004). Embryos were staged according to the number of embryonic days (E). Gut stages were referenced to the chick embryo gut staging table (Southwell, 2006) and the ENS formation timetable (Allan and Newgreen, 1980).

Wnt1-Cre mice (*Tg(Wnt1Cre)11Rth Tg(Wnt1-GAL4)11Rth/J*, Stock #003829) were crossed with R26R-tdT reporter mice (B6.Cg-*Gt(ROSA)26Sortm14(CAG-tdTomato)Hze*/J, Stock #007914) to obtain Wnt1-Cre;tdTomato (Wnt1;tdT) mice. Mice were sacrificed by cervical dislocation and embryos were dissected from the decidua in serum-free DMEM medium (Sigma). The day of the vaginal plug was considered 0.5 days post-coitum. Avian embryo experiments were approved by the Institutional Animal Care and Use Committees of Semmelweis University, Royal Children's Hospital Animal Ethics Committee, permits A596 and A650, and MCRI Institutional Biosafety Committee Certificate 127. Mouse experiments were approved by the Institutional Animal Care and Use Committee at Massachusetts General Hospital.

Intestinal organ culture assay to induce enteric ganglioneuromas

Intestines were dissected from E6-E9 chick and E11.5 C57BL/6 or Wnt1;tdT mouse embryos. The intestines were placed in catenary culture either by attaching their ends to a V-shaped piece of Millipore paper with the majority of the gut hanging in the middle (Hao et al., 2019; Hearn et al., 1999) or by pinning the gut to a silicone-coated Petri dish as described previously (Nagy et al., 2016). Gut was cultured in DMEM (Sigma), 1% glutamine, 1% penicillin/streptomycin antibiotic mixture (Invitrogen), with or without added GDNF (40 ng/ml; R&D Systems, Recombinant Human GDNF, cat. no: 212-GD-010) for 48-72 hours.

To study the effect of GDNF concentration and treatment duration on ganglioneuroma formation and hindgut ENS colonization, E7 chick intestines were cultured in the presence of GDNF (10, 40, 100 and 500 ng/ml) for 72 hours. The length of aganglionic hindgut was measured at the end of the culture period (n=6 guts per GDNF concentration tested). To compare ganglioneuroma size and number among the treatment groups (n=6 guts per group), guts were photographed at 24, 48, and 72 hours. The diameter of 10 ganglioneuromas was measured using NIS-Elements BR 5.02 software. Ganglioneuroma number was determined by counting all the tumors and dividing by the gut length in mm. Statistical comparisons were made using ANOVA with Tukey's multiple comparisons test. A p-value <0.05 was considered significant.

Quantification of ENS cell number and neuronal differentiation was performed by culturing E6.5 chick intestine for 2 days in catenary conditions with (n=3) or without (n=3) added GDNF (40 ng/ml). Wholemounts were immunolabelled with antibodies to Hu and SoxE, then transverse sections obtained through the mid-hindgut. For convenience, the circular hindgut sections were divided into counting units of nine equal pie-segments, each comprising 40° of arc. The number of neurons (HuC/D+) and non-neuronal ENCCs (SoxE+) were counted in the submucosal plexus of each segment. Statistical analysis was performed using one-way ANOVA with Fisher's Least Significant Difference (LSD) post-test.

Vagal and sacral neural crest electroporation

The transposon-containing pT2K-CAGGS-GFP expression construct encoding EGFP, and the pCAGGS-T2TP expression construct encoding transposase (Sato et al., 2007) were kind gifts of Prof. Y. Takahashi, Nara, Japan. These were prepared using a QIAfilter Plasmid Midi kit (12243; QIAGEN, Hilden, Germany) and resuspended together in water at 1.25-2.5 µg/µL each (Simkin et al., 2014). For vagal level electroporation, chick embryos of E1.5 (7-10 somites) were exposed *in ovo* and the plasmid mixture was injected into the neural tube lumen at the vagal level. Electrical parameters were three 10-12V, 50 msec pulses delivered bilaterally at one second intervals, using a custom-built electroporator (Scott Fraser, Univ. of Southern California) with gold electrodes. For sacral level electroporation, embryos were E2.25 (22-24 somites) and the plasmid mixture was injected into the neural tube caudal to the last somite with voltage of 25V. After electroporation, the eggs were sealed and re-incubated until E6.5-7 (Simkin et al., 2014).

Transplantation to preganglionic embryonic chick hindgut

Chimeric experiments were performed as described previously. GDNF-induced enteric ganglioneuromas were harvested from either GFP-chick or Wnt1;tdT mouse with fine forceps and one ganglioneuroma was transplanted into each of the two ceca of an isolated preganglionic hindgut of an E5 chick embryo under stereomicroscope visualization (Nagy et al., 2018). Hindguts were then cultured on the chorioallantoic membrane (CAM) of E9 host chick embryos for 9 days (n=9), then processed for immunofluorescence. The graft, together with the surrounding CAM, was excised, fixed in 4% paraformaldehyde (PFA), and embedded for cryosectioning.Dissociated ganglioneuroma cultureSingle cell suspensions of E11.5 Wnt1;tdT derived ganglioneuromas (n=7) were transferred to glass-bottom chamber

slides (Ibidi, Germany) coated with 20 µg/ml fibronectin (Sigma) and cultured for a further two days in DMEM medium containing GDNF. 5-ethynyl-20-deoxyuridine (EdU; 10 µM) was added to the culture medium 24 hours prior to fixation with 4% PFA and processed for Tuj1 immunofluorescence staining.Immunofluorescence stainingTissue samples were fixed for 1 hour in 4% PFA, then infiltrated with 15% sucrose in PBS overnight at 4°C. The medium was changed for 7.5% gelatin (Sigma) containing 15% sucrose and the tissues rapidly frozen at -50°C in 2-methylbutane (Sigma). Frozen sections were cut at 12 µm, collected on poly-L-lysine–coated slides (Sigma), and stained by immunocytochemistry as previously described (Nagy and Goldstein, 2006). The following primary antibodies were used: goat anti-RET (cat. no: GT15002, 1:20, Neuromics, Edina, MN); p75 (cat. no: G3231, Promega), which recognizes the cytoplasmic domain of the p75 neurotrophin receptor on the surface of migratory and postmigratory neural crest-derived cells; anti-SoxE (Sox-8,9 and 10, kind gift of Craig Smith, Monash University); anti-HuC/D (clone: 16A11, ThermoFisher), which recognizes a neuron-specific RNA-binding protein; anti-Tuj1 (clone: B1195, Covance), a neuron-specific class III beta-tubulin, mouse anti-Neurofilament (clone: 2F11, 1:50, NeoMarkers, Fremont, CA), rabbit anti-PGP9.5 (cat. no: CL7756AP-50, 1:400, Cedarlane, Burlington, NC), rabbit anti-neuronal nitric oxide synthase (cat. no: 61-7000, nNOS; 1:200, Thermo Fisher); rabbit anti-synaptophysin (cat no: ab14692, 1:100, Abcam); BFABP (brain fatty acid binding protein, Kurz et al., 1994); rabbit anti-S100B calcium binding protein B (cat no: RB087A1, S100; 1:50; NeoMarkers, Fremont, CA), GFAP (clone: Z0334, Glial fibrillary acidic protein, DAKO) to detect the early and differentiated enteric glia; fibronectin (clone: B3/D6) and tenascin-C (clone: MI-B4) antibodies were obtained from the Developmental Studies Hybridoma Bank (DSHB, Iowa, USA); anti-alpha smooth muscle actin (SMA; clone:1A4, NeoMarkers); anti-GFP (cat. no: 600-101-215M, green florescent protein, Rockland); and CN, a chicken-specific neurite marker (Kuratani and Tanaka, 1990). After rehydration in PBS, sections were incubated with primary antibodies for 45 minutes, followed by Alexa-conjugated fluorescent secondary antibodies: Alexa Fluor 488 goat anti-mouse IgG, Alexa Fluor 594 goat anti-mouse IgG, Alexa Fluor 546 goat anti-rabbit IgG, and Alexa Fluor 488 goat anti-rabbit IgG (ThermoFisher). Nuclei were stained with DAPI.

For wholemount immunolabeling, specimens were treated with 0.05% trypsin (10 min. at room temperature), fixed in 4% PFA for 1 hour, then blocked and permeabilized with 1% horse serum and 0.1% Triton X-100 in PBS. Specimens were labelled overnight with primary antibodies (GFP, HuC/D or SOXE). After washing in PBS, species-specific secondary

antibodies and streptavidin:AMCA were applied overnight (Simpson et al., 2007). After further washing in PBS, wholemounts were mounted in Vectashield (Vector Laboratories, CA, USA) between two coverslips. After images were taken, wholemounts were demounted, frozen in Tissu-Tek, sectioned transversely at 16 μm, and mounted on microscope slides. In some cases, sections were re-labelled with HuC/D antibody followed by secondary antibody. Wholemount images were recorded with a Leica M205 FA fluorescence stereomicroscope, and wholemount and section images were recorded with an Olympus IX70 fluorescence microscope. Image processing used Leica and Zeiss proprietary software, QCapture Pro, and ImageJ.

Cell proliferation

For cell proliferation, EdU (ThermoFisher) was added to culture medium three hours prior to 4% PFA fixation. EdU incorporation was detected using the Click-iT EdU Imaging Kit (ThermoFisher). Sections were examined under a Nikon Microphot FXA microscope and digital images captured with a Spot camera and software version 3.3.1 (Diagnostic Instruments). Images were compiled using Adobe Photoshop 7.0.

Funding

A.M.G. is supported by the National Institutes of Health (R01DK103785). N.N. is supported by a Bolyai Fellowship from the Hungarian Academy of Sciences, Excellence Program for Higher Education of Hungary (FIKP), and Hungarian Science Foundation NKFI grant (124740). R.A.G. is supported by the National Institutes of Health (F32DK121440)

References

Akbareian, S. E., Nagy, N., Steiger, C. E., Mably, J. D., Miller, S. A., Hotta, R., Molnar, D. and Goldstein, A. M. (2013). Enteric neural crest-derived cells promote their migration by modifying their microenvironment through tenascin-C production. *Dev. Biol.* **382**, 446–456.

Allan, I. J. and Newgreen, D. F. (1980). The origin and differentiation of enteric neurons of the intestine of the fowl embryo. *Am. J. Anat.* **157**, 137–154.

Amiel, J., Sproat-Emison, E., Garcia-Barcelo, M., Lantieri, F., Burzynski, G., Borrego, S., Pelet, A., Arnold, S., Miao, X., Griseri, P., et al. (2008). Hirschsprung disease, associated syndromes and genetics: a review. *J. Med. Genet.* **45**, 1–14.

Arighi, E., Popsueva, A., Degl'Innocenti, D., Borrello, M. G., Carniti, C., Perälä, N. M., Pierotti, M. A. and Sariola, H. (2004). Biological Effects of the Dual Phenotypic Janus Mutation of ret Cosegregating with Both Multiple Endocrine Neoplasia Type 2 and Hirschsprung's Disease. *Mol. Endocrinol.* **18**, 1004–1017.

Arighi, E., Borrello, M. G. and Sariola, H. (2005). RET tyrosine kinase signaling in development and cancer. *Cytokine Growth Factor Rev.* **16**, 441–467.

Brodeur, G. M. (2018). Spontaneous regression of neuroblastoma. *Cell Tissue Res.* **372**, 277–286.

Brooks, A. S., Oostra, B. A. and Hofstra, R. M. W. (2005). Studying the genetics of Hirschsprung's disease: unraveling an oligogenic disorder. *Clin. Genet.* **67**, 6–14.

Cohen, M. S., Phay, J. E., Albinson, C., DeBenedetti, M. K., Skinner, M. A., Lairmore, T. C., Doherty, G. M., Balfe, D. M., Wells, S. A. and Moley, J. F. (2002). Gastrointestinal Manifestations of Multiple Endocrine Neoplasia Type 2: *Ann. Surg.* **235**, 648–655.

Eng, C., Clayton, D., Schuffenecker, I., Lenoir, G., Cote, G., Gagel, R. F., Amstel, H. K. P. van, Lips, C. J. M., Nishisho, I., Takai, S.-I., et al. (1996). The Relationship Between Specific RET Proto-oncogene Mutations and Disease Phenotype in Multiple Endocrine Neoplasia Type 2: International RET Mutation Consortium Analysis. *JAMA* **276**, 1575–1579.

Erdogan, M. F., Gulec, B., Gursoy, A., Pekcan, M., Azal, O., Gunhan, O. and Bayer, A. (2006). Multiple endocrine neoplasia 2B presenting with pseudo-Hirschsprung's disease. *J. Natl. Med. Assoc.* **98**, 783–786.

Goldstein, A., Hofstra, R. and Burns, A. (2013). Building a brain in the gut: development of the enteric nervous system. *Clin. Genet.* **83**, 307–316.

Hansford, J. R. and Mulligan, L. M. (2000). Multiple endocrine neoplasia type 2 and RET: from neoplasia to neurogenesis. *J. Med. Genet.* **37**, 817–827.

Hao, M. M., Bergner, A. J., Newgreen, D. F., Enomoto, H. and Young, H. M. (2019). Technologies for Live Imaging of Enteric Neural Crest-Derived Cells. *Methods Mol. Biol. Clifton NJ* **1976**, 97–105.

Hearn, C. J., Young, H. M., Ciampoli, D., Lomax, A. E. G. and Newgreen, D. (1999). Catenary cultures of embryonic gastrointestinal tract support organ morphogenesis, motility, neural crest cell migration, and cell differentiation. *Dev. Dyn.* **214**, 239–247.

Hechtman, J. F. and Harpaz, N. (2015). Neurogenic Polyps of the Gastrointestinal Tract: A Clinicopathologic Review With Emphasis on Differential Diagnosis and Syndromic Associations. *Arch. Pathol. Lab. Med.* **139**, 133–139.

Heuckeroth, R. O., Lampe, P. A., Johnson, E. M. and Milbrandt, J. (1998). Neurturin and GDNF Promote Proliferation and Survival of Enteric Neuron and Glial Progenitorsin Vitro. *Dev. Biol.* **200**, 116–129.

Kuratani, S. and Tanaka, S. (1990). Peripheral development of avian trigeminal nerves. *Am. J. Anat.* **187**, 65–80.

Matthay, K. K., Maris, J. M., Schleiermacher, G., Nakagawara, A., Mackall, C. L., Diller, L. and Weiss, W. A. (2016). Neuroblastoma. *Nat. Rev. Dis. Primer* **2**, 1–21.

McGrew, M. J., Sherman, A., Ellard, F. M., Lillico, S. G., Gilhooley, H. J., Kingsman, A. J., Mitrophanous, K. A. and Sang, H. (2004). Efficient production of germline transgenic chickens using lentiviral vectors. *EMBO Rep.* **5**, 728–733.

Menko, F. H., van der Luijt, R. B., de Valk, I. A. J., Toorians, A. W. F. T., M. Sepers, J., van Diest, P. J. and Lips, C. J. M. (2002). Atypical MEN Type 2B Associated with Two Germline RET Mutations on the Same Allele Not Involving Codon 918. *J. Clin. Endocrinol. Metab.* **87**, 393–397.

Moore, S. W. and Zaahl, M. (2010). Familial associations in medullary thyroid carcinoma with Hirschsprung disease: the role of the RET-C620 "Janus" genetic variation. *J. Pediatr. Surg.* **45**, 393–396.

Mulligan, L. M., Kwok, J. B. J., Healey, C. S., Elsdon, M. J., Eng, C., Gardner, E., Love, D. R., Mole, S. E., Moore, J. K., Papi, L., et al. (1993). Germ-line mutations of the RET proto-oncogene in multiple endocrine neoplasia type 2A. *Nature* **363**, 458–460.

Nagy, N., Brewer, K. C., Mwizerwa, O. and Goldstein, A. M. (2007). Pelvic plexus contributes ganglion cells to the hindgut enteric nervous system. *Dev. Dyn.* **236**, 73–83.

Nagy, N., Burns, A. J. and Goldstein, A. M. (2012). Immunophenotypic characterisation of enteric neural crest cells in the developing avian colorectum. *Dev. Dyn. Off. Publ. Am. Assoc. Anat.* **241**, 842–851.

Nagy, N., Barad, C., Graham, H. K., Hotta, R., Cheng, L. S., Fejszak, N. and Goldstein, A. M. (2016). Sonic hedgehog controls enteric nervous system development by patterning the extracellular matrix. *Development* **143**, 264–275.

Nagy, N., Barad, C., Hotta, R., Bhave, S., Arciero, E., Dora, D. and Goldstein, A. M. (2018). Collagen 18 and agrin are secreted by neural crest cells to remodel their microenvironment and regulate their migration during enteric nervous system development. *Dev. Camb. Engl.* **145**,.

Plaza-Menacho, I., Sluis, T. van der, Hollema, H., Gimm, O., Buys, C. H. C. M., Magee, A. I., Isacke, C. M., Hofstra, R. M. W. and Eggen, B. J. L. (2007). Ras/ERK1/2-mediated STAT3 Ser727 Phosphorylation by Familial Medullary Thyroid Carcinoma-associated RET Mutants Induces Full Activation of STAT3 and Is Required for c-fos Promoter Activation, Cell Mitogenicity, and Transformation. *J. Biol. Chem.* **282**, 6415–6424.

Read, R. D., Goodfellow, P. J., Mardis, E. R., Novak, N., Armstrong, J. R. and Cagan, R. L. (2005). A Drosophila Model of Multiple Endocrine Neoplasia Type 2. *Genetics* **171**, 1057–1081.

Romeo, Ceccherini, Celli, Priolo, Betsos, Bonardi, Seri, Yin, Lerone, Jasonni, et al. (1998). Association of multiple endocrine neoplasia type 2 and Hirschsprung disease. *J. Intern. Med.* **243**, 515–520.

Sato, Y., Kasai, T., Nakagawa, S., Tanabe, K., Watanabe, T., Kawakami, K. and Takahashi, Y. (2007). Stable integration and conditional expression of electroporated transgenes in chicken embryos. *Dev. Biol.* **305**, 616–624.

Simkin, J. E., Zhang, D., Ighaniyan, S. and Newgreen, D. F. (2014). Parameters affecting efficiency of in ovo electroporation of the avian neural tube and crest. *Dev. Dyn.* **243**, 1440–1447.

Simpson, M. J., Zhang, D. C., Mariani, M., Landman, K. A. and Newgreen, D. F. (2007). Cell proliferation drives neural crest cell invasion of the intestine. *Dev. Biol.* **302**, 553–568.

Smith, V. V., Eng, C. and Milla, P. J. (1999). Intestinal ganglioneuromatosis and multiple endocrine neoplasia type 2B: implications for treatment. *Gut* **45**, 143–146.

Southwell, B. R. (2006). Staging of intestinal development in the chick embryo. *Anat. Rec. A. Discov. Mol. Cell. Evol. Biol.* **288A**, 909–920.

Takahashi, M., Iwashita, T., Santoro, M., Lyonnet, S., Lenoir, G. M. and Billaud, M. (1999). Co-segregation of MEN2 and Hirschsprung's disease: The same mutation of RET with both gain and loss-of-function? *Hum. Mutat.* **13**, 331–336.

Taraviras, S., Marcos-Gutierrez, C. V., Durbec, P., Jani, H., Grigoriou, M., Sukumaran, M., Wang, L. C., Hynes, M., Raisman, G. and Pachnis, V. (1999). Signalling by the RET receptor tyrosine kinase and its role in the development of the mammalian enteric nervous system. *Development* **126**, 2785–2797.

Vidal, M., Wells, S., Ryan, A. and Cagan, R. (2005). ZD6474 suppresses oncogenic RET isoforms in a Drosophila model for type 2 multiple endocrine neoplasia syndromes and papillary thyroid carcinoma. *Cancer Res.* **65**, 3538–3541.

Young, H. M., Hearn, C. J., Farlie, P. G., Canty, A. J., Thomas, P. Q. and Newgreen, D. F. (2001). GDNF Is a Chemoattractant for Enteric Neural Cells. *Dev. Biol.* **229**, 503–516.

Young, H. M., Bergner, A. J. and Müller, T. (2003). Acquisition of neuronal and glial markers by neural crest-derived cells in the mouse intestine. *J. Comp. Neurol.* **456**, 1–11.

Figures

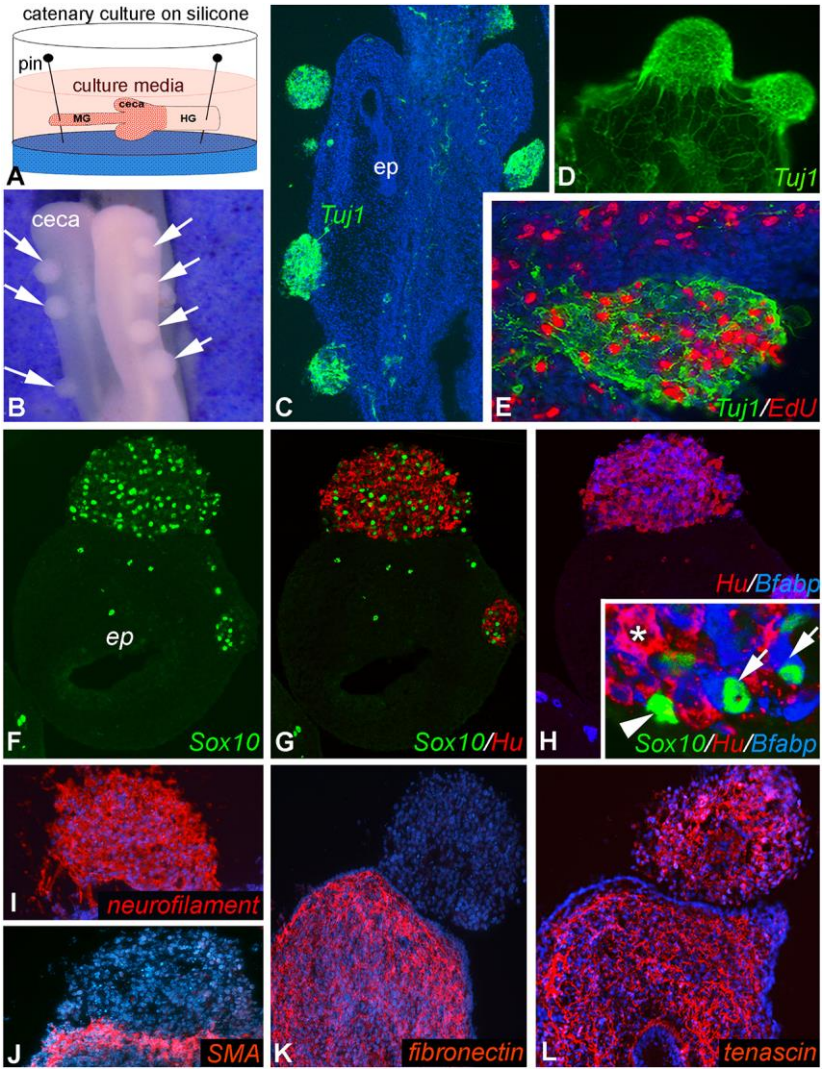

Figure 1. Exogenous GDNF leads to ectopic ENCC aggregates in chick intestine. The intestine was explanted from E7 chick and placed in catenary culture for 48 hours (A). Addition of exogenous GDNF protein induced ENCCs to form aggregates on the surface of the midgut and ceca (B, arrows). Cells in the aggregates express neuronal markers Tuj1 (C-E), Hu (G,H), and neurofilament (I). Sox10 expression labels ENCC progenitors and glial cells (F-H). The glia are marked by co-expression of Sox10 and BFABP (H, inset, arrows), while progenitors are Sox10+/BFABP- (H, inset, arrowhead). SMA is not present in the aggregates (J). They also express tenascin-C (L), but not fibronectin (K). Active cellular proliferation was present in the ENCC aggregates (E).

ep, epithelium; hg, hindgut; mg, midgut

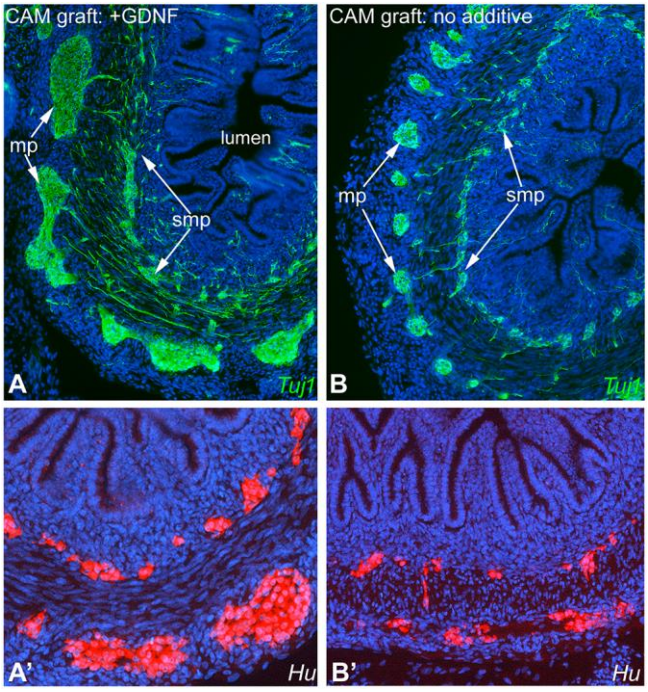

Figure 2. GDNF treatment leads to enteric hyperganglionosis. To observe the development of the aggregates over a prolonged time, E6 midgut was cultured in the presence of GDNF for 48 hours and then transplanted onto the CAM of a host chick embryo for an additional seven days. Significant hyperganglionosis is seen in the submucosal and myenteric plexuses of GDNF-treated guts (A,A') as compared to normal, untreated controls (B,B'). mp, myenteric plexus; smp, submucosal plexus

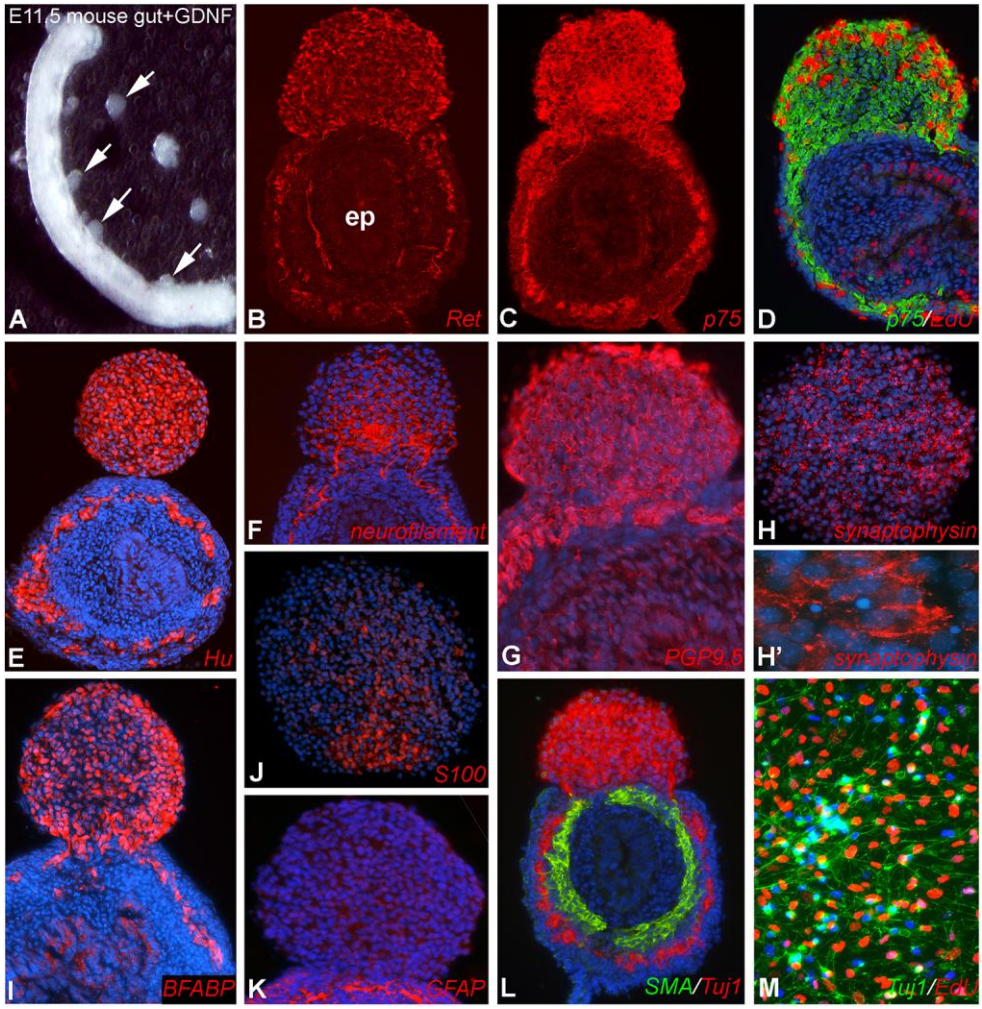

Figure 3. Exogenous GDNF leads to ENCC aggregates in mouse intestine. The intestine was explanted from E11.5 mouse and cultured with GDNF for 48 hours. GDNF induced ENCCs to form aggregates on the surface of the intestine (A, arrows). Cells in the aggregates express neural crest (B-D) and neuronal (E-H') markers, BFABP (I) and S100 (J), but not GFAP (K) or SMA (L). ENCCs from dissociated aggregates showed active cellular proliferation (M).

ep, epithelium

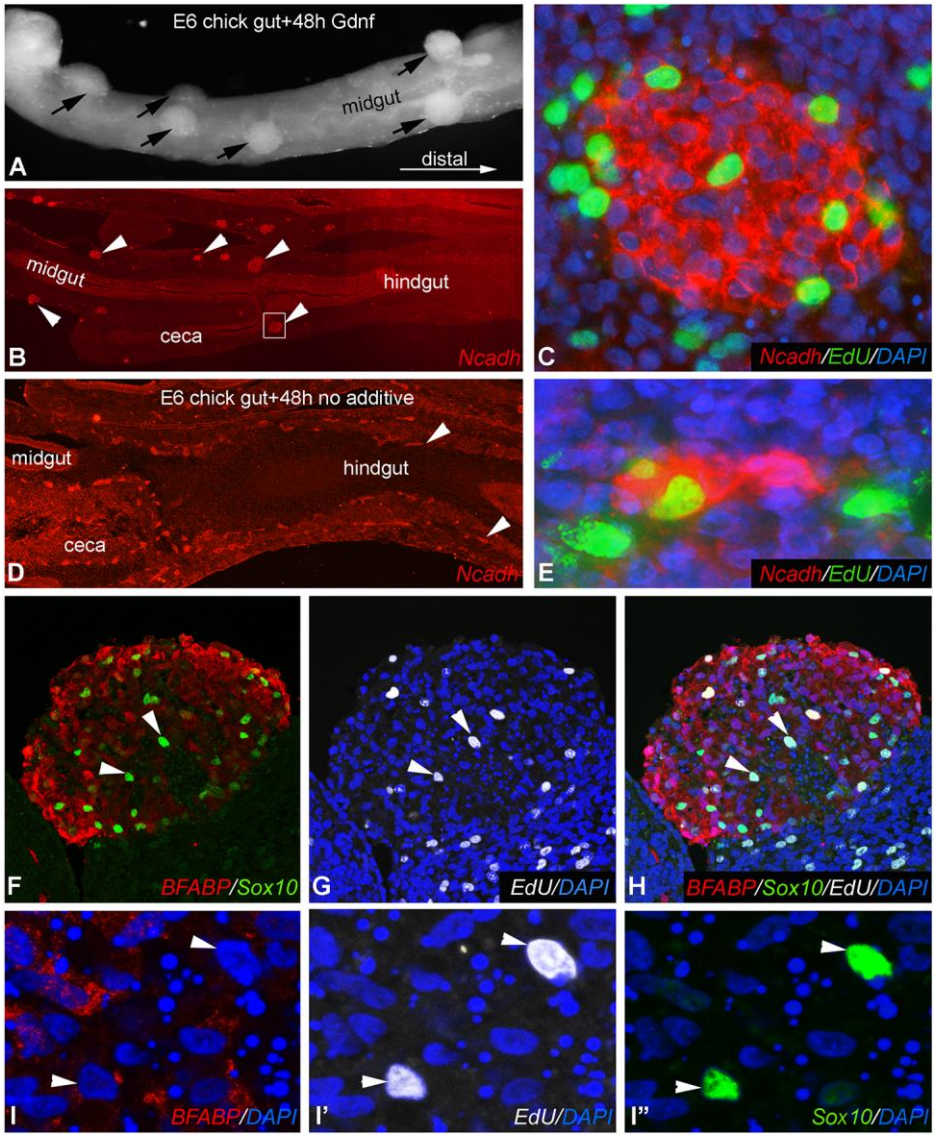

Figure 4. GDNF treatment of embryonic chick gut leads to migratory arrest of ENCCs associated with accelerated neuronal differentiation. E6 chick gut cultured in GDNF for 48 hours resulted in cellular aggregates in the midgut (A, arrows) and arrested migration of ENCCs in the proximal hindgut (B, arrowheads mark Ncadh+ ENCCs). Cell aggregates formed both on (A) and within (B) the intestine, with EdU incorporation in Ncadh+ cells indicating robust ENCC proliferation (C). Control E6 guts not treated with GDNF displayed unperturbed ENCC migration after 48 hours (D), no aggregates, and normal-sized enteric ganglia with occasional EdU+ cells (E). Within the GDNF-induced aggregates, many of the EdU+ cells are undifferentiated ENCCs that express Sox10, but not BFABP (F-H, arrowheads; magnified view of two such cells in I-I").

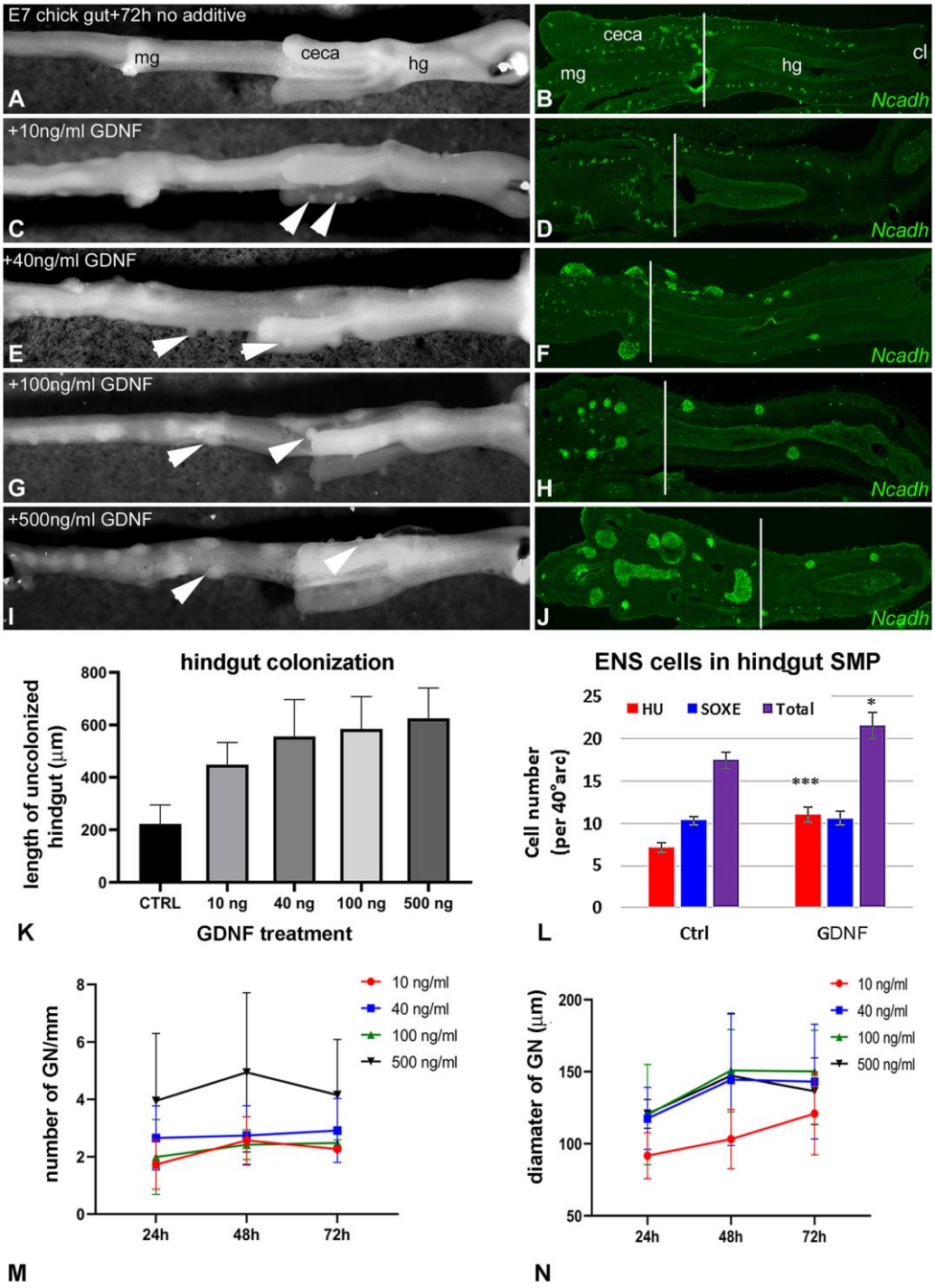

Figure 5. GDNF dosage is associated with size and number of ganglioneuromas and with extent of hindgut aganglionosis. E7 chick intestine was cultured for 72 hours in the presence of GDNF concentrations ranging from 0 to 500 ng/ml, n=6 per concentration, with wholemount images and longitudinal sections shown at the end of the incubation period (A-J; distal end is to the right). Higher GDNF concentration was associated with an increase in the length of hindgut aganglionosis (K; vertical lines mark midgut-hindgut junction; n=6 per group). The total number of ENCCs and their rate of neuronal differentiation were both higher

in hindguts treated with 40 ng/ml GDNF, n=3 per condition (L). GDNF concentration was also associated with ganglioneuroma number (M) and size (N), n=6 per time point. ANOVA with Tukey's multiple comparisons test used for K,M,N; ANOVA with Fisher's LSD post-test used in L. All data presented as mean +/- standard deviation.

GN, ganglioneuroma; mg, midgut; hg, hindgut; SMP, submucosal plexus

*p<0.05, ***p<0.001 versus control

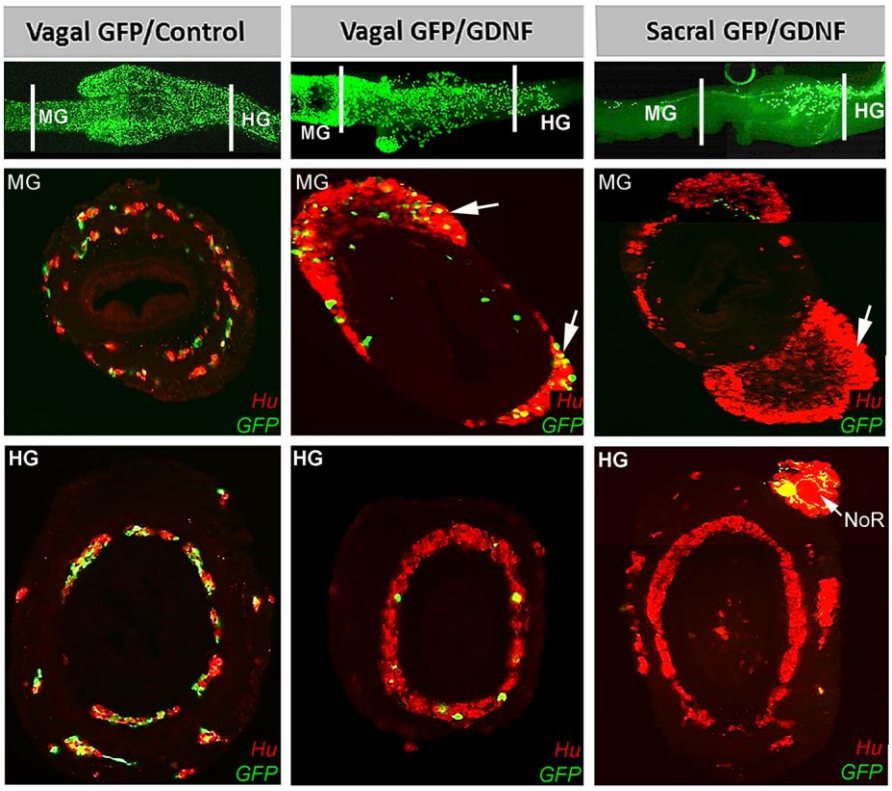

Figure 6. Vagal neural crest-derived cells give rise to GDNF-induced enteric ganglioneuromas. GFP-expressing plasmid was electroporated into the vagal neural tube at E1.5, and into the sacral neural tube at E2.25. The intestine was removed at E6.5-E7 and cultured for an additional 2 days. Compared to control intestine (left column), addition of GDNF caused large aggregates with many double-immunoreactive GFP+/Hu+ neurons to form on the periphery of the intestine at the midgut (MG) and cecal levels (middle column, arrows). These ganglioneuromas arise from vagal-derived ENCCs since they possess GFP+ cells after vagal neural tube electroporation (middle column, arrows). After sacral neural tube electroporation, the gangioneuromas (right column, arrow), are GFP-negative. GDNF also caused disorganization and loss of ENS cells in the submucosal and myenteric plexuses (middle row). The effect of exogenous GDNF on the hindgut (HG) ENS was less pronounced (bottom row). Three replicates of this experiment were conducted with the same result. HG, hindgut; MG, midgut; NoR, nerve of Remak

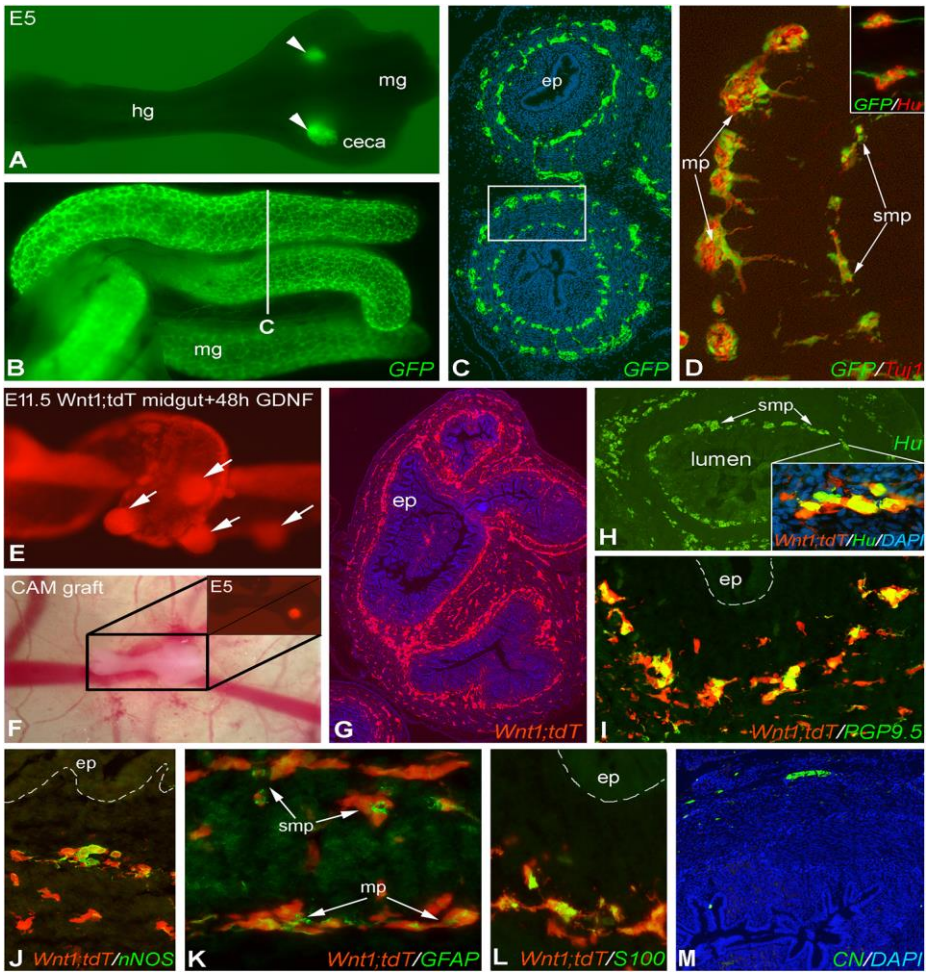

Figure 7. GDNF-induced ganglioneuromas in chick and mouse gut have the developmental potency to colonize the embryonic ENS. Intestines were isolated from E6 GFP-chick and E11.5 Wnt1;tdT mouse embryos and cultured with GDNF for 48 hours to form ganglioneuromas. Two GFP+ ganglioneuromas were removed from GFP-chick intestine implanted into the ceca of an E5 preganglionic chick hindgut (A, arrowheads), which was cultured on an E9 host CAM for 9 days. GFP+ ganglioneuromas give rise to a GFP+ ENS (B, labelled cross-section shown in C), containing a network of Tuj1+ (D) and Hu+ (D, inset) enteric neurons. Two ganglioneuromas were harvested from Wnt1;tdT mouse intestine (E) and one implanted into each ceca of an E5 chick gut and cultured on the CAM for 9 days (F). Wnt1+ tdT-expressing cells migrate throughout the hindgut to form submucosal and myenteric plexuses (G) that express neuron-specific Hu (H), PGP9.5 (I), and nNOS (J). The Wnt1+ cells also express the glial markers GFAP (K) and S100 (L), but not chick-specific CN antibody (M), confirming their mouse origin.

ep, epithelium; hg, hindgut; mg, midgut; mp, myenteric plexus; smp, submucosal plexus

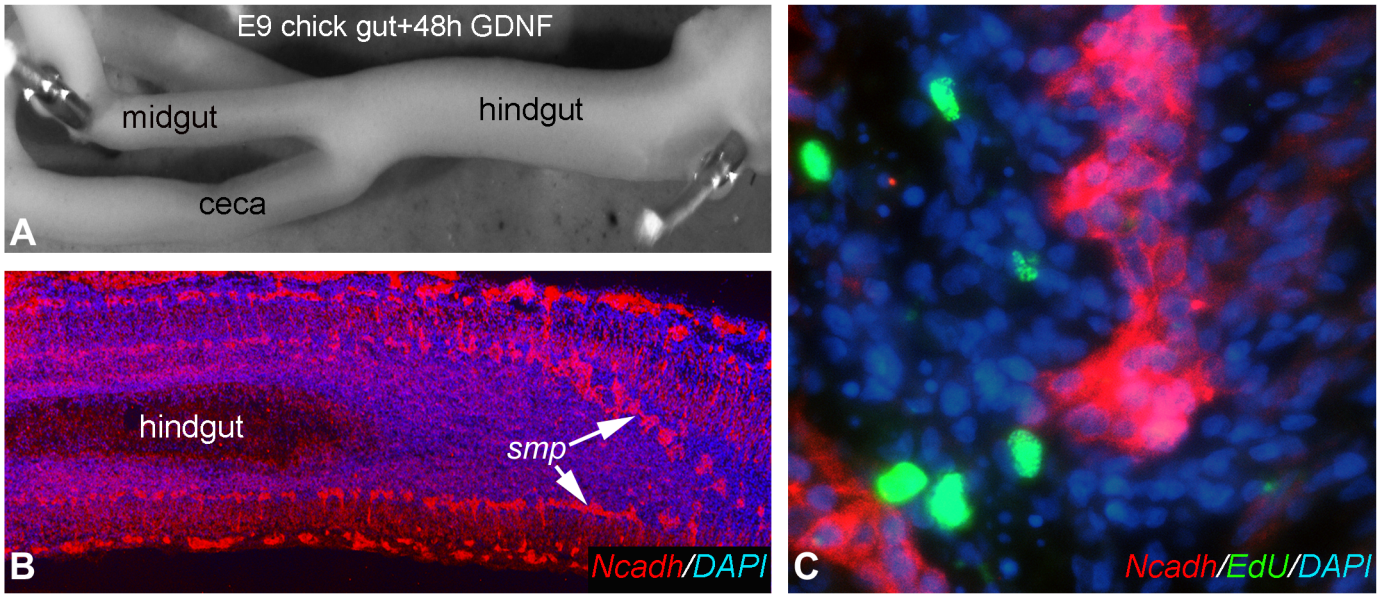

Figure S1. The ability of GDNF to induce ganglioneuroma formation is time-limited. Addition of GDNF to explanted E9 intestine did not result in cell aggregate formation (A) and did not disrupt ENCC migration (B). Furthermore, EdU+ ENCCs were rarely observed (C).

smp, submucosal plexus

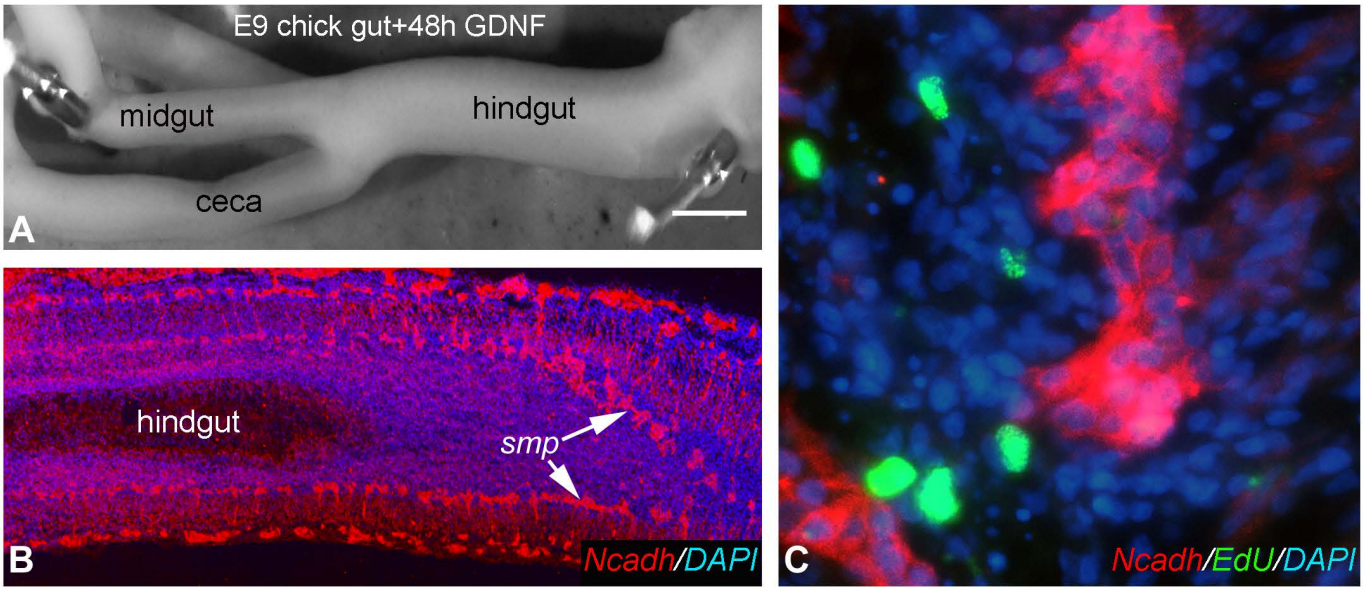

Figure S1. The ability of GDNF to induce ganglioneuroma formation is time-limited. Addition of GDNF to explanted E9 intestine did not result in cell aggregate formation (A) and did not disrupt ENCC migration (B). Furthermore, EdU+ ENCCs were rarely observed (C). smp, submucosal plexus. Scale bar in A: 500 μm in A; 200 μm in B; 27 μm in C.